HHS Public Access

Author manuscript

Urology. Author manuscript; available in PMC 2015 October 01.

Published in final edited form as:

Urology. 2014 October ; 84(4): 982.e9–982.14. doi:10.1016/j.urology.2014.06.021.

Robotic-Assisted Fluorescence Sentinel Lymph Node Mapping Using Multi-Modal Image-Guidance in an Animal Model

Michael A. Liss, M.D.[a,b], **Sean P. Stroup**[c], **Zhengtao Qin Cand, Ph.D.**[d,e,f], **Carl Hoh, MD**[b,d,e,g], **David J. Hall, Ph.D.**[d,e], **David R. Vera, Ph.D.**[b,d,e,g], and **Christopher J. Kane, M.D.**[a,b,g]

[a]Department of Urology, UC San Diego Health System, San Diego, California

[b]UC San Diego Moores Cancer Center, La Jolla, California

[c]Naval Medical Center, San Diego, California

[d]Department of Radiology, University of California, San Diego, La Jolla, California

[e]UCSD In Vivo Cancer and Molecular Imaging Center, University of California, San Diego, La Jolla, California

[f]Department of Chemistry and Biochemistry, University of California, San Diego, La Jolla, California

[g]Department of Surgery, University of California, San Diego, La Jolla, California

Abstract

Objectives—To investigate PET/CT pre-operative imaging and intraoperative detection of a fluorescent-labeled receptor-targeted radiopharmaceutical in a prostate cancer animal model.

Methods—Three male Beagle dogs underwent an intra-prostatic injection of fluorescent-tagged tilmanocept radio-labeled with both gallium-68 and technetium-99m. One hour after injection a pelvic PET/CT scan was performed for pre-operative sentinel lymph node (SLN) mapping. Definition of SLN was a standardized uptake value (SUV) that exceeded 5% of the lymph node with the highest SUV. Thirty-six hours later we performed robotic-assisted SLN dissection using a fluorescence-capable camera system. Fluorescent lymph nodes were clipped, the abdomen was opened, and the pelvic and retroperitoneal nodes were excised. All excised nodal packets were assayed by *in vitro* nuclear counting and reported as percent-of-injected dose.

Corresponding Author: Christopher J. Kane, MD, UC San Diego Moores Cancer Center, 3855 Health Sciences Drive #0987, La Jolla, CA 92093-0987, Tel: (619) 543-2626, FAX: (619) 543-6573.

Financial/Conflict of Interest disclosures: David Vera Ph.D. is the inventor of Tilmanocept. Christopher Kane, M.D. and Sean Stroup, M.D., are consultants and have received honoraria from Intuitive Surgical, Inc.

Disclaimer: The views and opinions of, and endorsements by the author(s) do not necessarily reflect those of the U.S. Navy or the Department of Defense.

Results—Pre-operative PET/CT imaging identified a median of three sentinel lymph nodes per animal. All sentinel lymph nodes (100%) identified by the PET/CT were fluorescent during robotic-assisted lymph node dissection. Of all fluorescent nodes visualized by the camera system, 83% (10/12) satisfied the 5%-rule defined by the PET/CT scan. The two lymph nodes that did not qualify accumulated less than 0.002% of the injected dose.

Conclusions—Fluorescent-labeled tilmanocept has optimal logistical properties to obtain pre-operative PET/CT and subsequent real-time intraoperative confirmation during robotic-assisted sentinel lymph node dissection.

Keywords

Prostate Cancer; Fluorescence imaging; PET/CT imaging; multi-modal imaging; molecular imaging; sentinel lymph node

Introduction

Considerable variation exists regarding the decision to perform pelvic lymph node dissection (PLND) during radical prostatectomy for prostate cancer, as well as the extent of PLND.[1–3] Current risk calculators underestimate the risk of positive lymph nodes.[3] However, positive lymph nodes are associated with high recurrence and progression and may benefit from adjuvant or early salvage therapy.[4, 5] European studies have shown sentinel lymph node (SLN) biopsy during prostatectomy can accurately predict subsequent positive lymph nodes.[6, 7] Incorporation into widespread use has been limited due to lack of an ideal radiopharmaceutical agent.

The FDA recently approved technetium-99m-labeled tilmanocept (generic name, Lymphoseek™) for lymphatic mapping of breast cancer and melanoma.[8–10] It has a molecular diameter of 7.5 nm and exhibits avid binding to the lymphocyte receptor CD206 with sub-nanomolar affinity.[11] The non-particulate nature of tilmanocept and its avid receptor binding permits rapid SLN accumulation and sustained retention. These attributes permit SLN imaging within minutes or many hours after injection,[9] although rapid uptake permits the use of gallium-68-tilmanocept for tomographic imaging of pelvic SLNs via PET/CT imaging.[12] The long SLN residence time permits the use of fluorescent-labeled tilmanocept for intra-operative conformation during robotic-assisted surgery. We propose that the most accurate method for SLN mapping of prostate cancer is a multi-modality scheme that employs the quantitative and three-dimensional attributes of hybrid PET/CT imaging and the high sensitivity of fluorescence visualization by an endoscopic camera.

In preparation for human testing, we investigated the use of near infra-red-labeled tilmanocept for SLN imaging using Intuitive Surgical's *FireFly*™ endoscope in a canine model. Our primary goal was to confirm the use of pre-operative PET/CT imaging and confirmation by fluorescent visualization during robotic-assisted SLN mapping as it would be used in human clinical trials.

Materials and Methods

Experimental Design

We designed a non-survival study using three male Beagle canines in order to mimic the logistical process of procedure and imaging prior to surgery. First, using transrectal ultrasound guidance we performed the prostate injection of tilmanocept tagged with a near infra-red fluorescent dye and radiolabeled with gallium-68, a PET imaging isotope, and technetium-99m, a gamma-emitting isotope with a 6-hour half-life. One hour after injection we performed hybrid PET/CT imaging of the dog's pelvis. Standard uptake values (SUVs) for each visible lymph node were calculated from the PET/CT images, and used to determine if a visible node qualifies as a sentinel lymph node. Thirty-six hours after the pre-operative imaging, the animal was anesthetized and instrumented using the *Da Vinci Si* surgical robot fitted with the FireFly™ endoscopic camera system. Based the pre-operative PET/CT images, the instruments and camera were positioned over each region that qualified as the location of a sentinel lymph node. If fluorescence was visualized, the lymph node was clipped. After all of the SLN basins were inspected, the animal was euthanized and an open incision was made. All pelvic and retroperitoneal lymph nodes were removed, labeled, and assayed for technetium-99m to calculate the amount of fluorophore and the percent-of-injected tilmanocept.

Animal Model

Under a protocol approved by the Institutional Animal Care and Use Committee, prostate sentinel node mapping was evaluated in three adult male beagle dogs. All dogs were fasted overnight per protocol prior to the procedures. The dogs were sedated by intramuscular injection of an acepromazine/buprenorphine (0.01 – 0.05 mg/kg, 0.01 mg/kg) cocktail. After placement of a cephalic vein catheter, the animals were maintained under sedation by propofol infusion for the Transrectal ultrasound and agent injection. The dog was awakened from the first procedure, taken to an approved holding area, and brought to the operative suite to undergo general anesthesia for robotic surgery.

Imaging Agent

The preparation and quality control of fluorescent-labeled tilmanocept has been previously described.[13] The *800CW*-tilmanocept preparation consisted of an average of 55 molecules of mannose, 8 molecules of the chelation site for radiolabeling, and 1.5 dye molecules per tilmanocept. Radiolabeling of *800CW*-tilmanocept used a two-step process,[14] where each of the gallium-68 and technetium-99m generator eluates were sequentially added to a buffered solution of *800CW*-tilmanocept. Quality control of the radiolabeled product required both fluorescence and radiochemical purities to be greater than 97%. Approximately 2 ml of the fluorescent-radiopharmaceutical was drawn into a 3-ml syringe. After attaching a 7 inch 22 gauge spinal needle, the volume in the syringe was adjusted to 1.5 ml while capturing the effluent from the needle with a sterile needle cap.

Transrectal Injection of Imaging Agent

After anesthesia, we placed the dog in left lateral decubitus position and inserted the transrectal probe (BK Medical, Peabody, MD, USA). A side fire trans-rectal probe and guide were placed as per usual format similar to fiducial marker placement. After lubricated insertion of the transrectal probe, the prostate was identified and measured with an average size of 8 cc. The needle guide was used to line up the right lobe of the prostate. The 0.75-ml dose [^{68}Ga][^{99m}Tc]800CW-tilmanocept (1.5 nmol, ~1.0 mCi ^{68}Ga, ~0.2 mCi ^{99m}Tc) was injected in the right lobe of the prostate aiming for mid-gland and peripheral gland, being careful not to inject beyond the prostatic capsule. A Foley catheter was used to drain the bladder of urine for improved image acquisition.

PET/CT Image Acquisition and SUV-Based SLN Criteria

Images of the prostate injection site and pelvic lymph nodes were acquired using a PET/CT (GE Healthcare, *Discovery VCT*). A scout CT was acquired to confirm that the prostate and lymph node basins were within the PET field-of-view. Two bed-positions were acquired to cover all of the pelvic lymph node basins. PET images (5 mins, 3-D mode, isotope selection set to “Ga-68”) were acquired at one hour after injection; each image was followed by a CT acquisition (~1 sec). Standard iterative reconstruction software was employed to produce trans-axial, coronal, and sagittal PET cross-sections, which were merged with the appropriate CT cross-sections to produce hybrid PET/CT images. SUVs for each visualized lymph node were calculated with G.E. *Volume-Viewer* software. Any lymph node with an SUV that exceeded 5% of the highest lymph node SUV was defined as a sentinel lymph node.

Sentinel nodes were defined by the 5% rule, which indicates that secondary lymph nodes are considered SLN if they have at least 5% of the radioactivity as the ex vivo counts per minute of the hottest node. This concept is commonly used in breast cancer as the 10% rule, however, here we chose 5% to increase our sensitivity.[15]

Robotic-Assisted Surgery and FireFly™ Fluorescence Imaging

Robotic-assisted SLN mapping was performed 36 hours after injection of gallium-68 and technetium-99m-labeled *800CW*-tilmanocept. After induction of anesthesia, insufflation was performed using the Veress needle and subsequent port placement followed standard trochar placement for prostatectomy; however only 2 robotic arms were utilized due to intra-abdominal spatial constraints. The camera was placed in the midline approximately 3 cm below the xyphoid in order to visualize nodes that may be out of the usual field of view. The 8 mm robotic ports were placed slightly lateral to anterior axillary line. Two assistant 12 mm ports were placed for retraction and assistance. Steep Trendelenburg position was utilized to allow the bowels to fall cephalad and away from the pelvis. The FireFly™ Fluorescence Image Endoscope was utilized as a component of the *DaVinci Si* Robotic surgical system (Intuitive Surgical, Sunnyvale, CA, USA). The endoscope uses near-infrared light with an 805 nm wavelength excitation laser source.

We reviewed the PET/CT scan for localization and started the dissection at the prostate to confirm fluorescence at the injection site. Subsequently, we used the PET/CT to guide us to the location of each basin that contained a sentinel lymph node and then used the FireFly™ fluorescence camera to confirm the SLN location. We modified the endoscope to remove all background white light; therefore, real-time dissection was not feasible. When a candidate lymph node was found, a surgical clip was used to tag this node for dissection. After completion of the robotic portion, the animal was euthanized. An open incision was made and all lymph nodes from the pelvis and retroperitoneum were removed and labeled for nuclear counting.

Nuclear Counting

After dissection, the nodal packets were placed in a plastic scintillation vials and assayed for radioactivity using a gamma well counter (100–200-keV window, Gamma 9000; Beckman Instruments, Fullerton, CA). We calculated the percent injected dose (%ID) of [^{99m}Tc] Tilmanocept by comparing the tissue counts with the counting standard. The counting standard was prepared from a known dilution of injected material.

Results

We identified 2, 4, and 3 individual sentinel lymph nodes via PET/CT scanning in each animal, respectively. A dominant node was identified in each of the 3 experiments, specifically the right common iliac, presacral, and para-arotic locations (Table 1). Using the 5%-rule, pre-operative PET/CT imaging identified a median of three sentinel lymph nodes per animal. Using the PET/CT scans as targets for dissection, the fluorescent lymph node was encountered within minutes of the dissection. All sentinel lymph nodes (100%) identified by the PET/CT 5%-rule were fluorescent during robotic-assisted lymph node dissection. Of all fluorescent nodes visualized by the camera system, 83% (10/12) satisfied the 5%-rule defined by the PET/CT scan. The two lymph nodes that did not qualify accumulated less than 0.002% of the injected dose.

We provide one experiment as an example to demonstrate the sequence of events. After anesthesia, the prostate ultrasound was obtained in the left lateral decubitus position similar to prostate biopsy or fiducial marker placement. The prostate size was measured with standard measurement technique obtaining values of 26.7 mm width, 21.2 mm height, 28.4 mm in length for a prostate volume of 8.41 cm^3 (Figure 1a). Subsequently we injected the radiopharmaceutical agent into the right lobe of the prostate (Figure 1b). A Foley catheter is placed and PET/CT image acquisition is obtained as described above. We found a dominant presacral lymph node noted on coronal, axial, and sagittal views (Figure 2a, 2b, and 2c, respectively). The animal was recovered and approximately 36 hours post injection was brought to the surgical suit. The bladder was elevated to investigate the injection site and confirm fluorescence and lymph node identification ensued with clipping the lymph nodes (Figure 3a and 3b) for identification and gamma counter verification of radiation (Video).

Discussion

We describe a successful preclinical model using the fluorescent-labeled radiopharmaceutical tilmanocept in order to perform preoperative lymph node mapping and subsequent robotic assisted dissection. Thirty-six hours prior to surgery prostate injection was performed with ultrasound guidance as could potentially occur in clinical practice. PET/CT scan imaging identified sentinel lymph nodes that were later targeted during surgery. Subsequent fluorescent visualization was used to confirm the PET/CT images and guide dissection. The use of current standard robotic camera and instruments were designed to simulate planned human studies.

Gallium-68 and technetium-99m-labeled *800CW*-tilmanocept is a novel, dual-labeled radio pharmaceutical with optimal logistical properties to obtain preoperative PET/CT and subsequent real-time intraoperative confirmation during robotic assisted SLN dissection. The procedure only requires one injection due to its lymph node binding properties, and will stay localized within the SLN for at least 36 hours. Actual binding to the lymph node is a feature that distinguishes our tilmanocept from indocyanine green (ICG) or other dyes, which only flows through lymph channels without stopping or binding. Moreover, tilmanocept allows preoperative PET/CT acquisition to identify the SLN site to direct dissection. Previous studies have noted reduced operative time in finding SLNs during radical prostatectomy with hand held gamma detectors and relative success at single instiutions.[16, 17, 18] Our study now provides a similar approach to SLN mapping preoperatively with the added benefit of real-time visual confirmation during robotic prostatectomy. Radiologic review was helpful in our series and once robotic dissection ensued, the fluorescent visualization confirmed the correct lymph node was obtained. In humans, this SLN would be sent to pathology for frozen section confirmation of metastasis, affecting the decision to either pursue extended PLND or determine that no further dissection is necessary.

PLND is a controversial topic in localized PCa despite a benefit recognized in a subset of patients.[19] Pelvic lymphadenectomy (PLND) during radical prostatectomy provides staging information that may guide adjuvant therapy; however the degree and extent of PLND remains a significant question in the surgical treatment of prostate cancer.[4, 20–24] An increase in low-grade low stage PCa has lead to a reduced risk of lymph node involvement and guidelines have adopted omission of PLND for these men.[1] Unfortunately, technology (robotic prostatectomy) rather than pathology has also impacted PLND decision-making.[25] When a PLND is indicated the anatomic extent is highly debated, which, may affect adherence to PCa guidelines.[26] Herein lies the true value of the SLN approach to PLND in that it can identify the highest risk location of the node even if it is in an aberrant location outside the usual dissection fields. Additionally, the SLN can be examined more closely with repeat sectioning or molecular-based tests, which could change management similar to the addition of molecular lymph node characterization in breast cancer staging.[27]

Current risk calculators are based on the historical reference of a limited or obturator PLND. Limited PLNDs resect only 35% of the lymph nodes draining the primary landing zones of the prostate, thereby potentially underestimating real risk.[28, 29] There has been a movement

toward more extensive lymphadenectomy in order to increase the sensitivity of lymphadenectomy. However, the more extensive node dissections are time consuming and potentially add some morbidity. A sentinel lymph node dissection (SLND) may allow improved detection of “at risk” lymph nodes while allowing a more limited and less morbid lymphadenectomy. Therefore, a potential solution to the PLND question could be performing an SLND.

The SLN mapping technique may reduce complications of increasingly extensive lymph node dissections (i.e., lymphocele, lymphedema, deep venous thrombosis, and pulmonary embolism) by limiting resection to first-order draining nodes.[30] The SLN mapping concept has been tested in over 1,000 prostatectomies noting only 1% of metastases were found in patients with negative SLN and improves detection over current EAU guidelines for extended PLND.[6, 18]. The risks of SLND are the potential morbidity of transrectal ultrasound guided needle injection of the fluorescent tilmanocept and the increased cost of using this technique. However, the improved staging information may play an ever increasing role in future management of prostate cancer and allow for improved categorization in clinical trials. Our study provides pilot data for FDA submission and subsequent planning for a human clinical trial regarding the utility of SLND.

Conclusion

Gallium-68 and technetium-99m-labeled *800CW*-tilmanocept has optimal logistical properties to obtain preoperative PET/CT and subsequent real-time intraoperative confirmation during robotic assisted sentinel lymph node dissection. Further phase 1–3 human clinical trials are needed to confirm the appropriate safety and subsequent clinical benefit of fluorescent labeled tilmanocept.

Supplementary Material

Refer to Web version on PubMed Central for supplementary material.

Acknowledgments

Funding/Support: This research was supported by the National Cancer Institute (P50 CA114745) and Intuitive Surgical (Sunnyvale, CA, U.S.A). Intuitive provided software modifications to the DaVinci Si robotic system and the FireFly™ endoscope adjustments. Otherwise they were not involved in the design, analysis, or writing of this study or manuscript.

The authors thank LiCOR Biosciences for supplying the *IRDye 800CW* NHS-ester dye and to Dr. Jonathan Sorger from Intuitive Surgical for his assistance with software modifications of the *DaVinci* robotic surgical system and continued support. This project was supported by the NIH/National Cancer Institute: In Vivo Molecular and Cancer Imaging Center grant (P50 CA114745).

References

1. Briganti A, Blute ML, Eastham JH, et al. Pelvic lymph node dissection in prostate cancer. Euro Urol. 2009; 55(6):1251–1265.
2. Touijer KA, Ahallal Y, Guillonneau BD. Indications for and anatomical extent of pelvic lymph node dissection for prostate cancer: practice patterns of uro-oncologists in North America. Urologic Oncol. 2013; 31(8):1517–1521. e1–2.

3. Yuh BE, Ruel NH, Mejia R, et al. Robotic extended pelvic lymphadenectomy for intermediate- and high-risk prostate cancer. Euro Urol. 2012; 61(5):1004–1010.
4. Messing EM, Manola J, Sarosdy M, et al. Immediate hormonal therapy compared with observation after radical prostatectomy and pelvic lymphadenectomy in men with node-positive prostate cancer. New Engl J Med. 1999; 341(24):1781–1788. [PubMed: 10588962]
5. Gervasi LA, Mata J, Easley JD, et al. Prognostic significance of lymph nodal metastases in prostate cancer. J Urol. 1989; 142(2 Pt 1):332–336. [PubMed: 2501518]
6. Winter A, Kneib T, Henke RP, et al. Sentinel lymph node dissection in more than 1200 prostate cancer cases: Rate and prediction of lymph node involvement depending on preoperative tumor characteristics. Intl J Urol. 2014; 21(1):58–63.
7. Holl G, Dorn R, Wengenmair H, et al. Validation of sentinel lymph node dissection in prostate cancer: experience in more than 2,000 patients. Eur J Nuclear Med Mol Imaging. 2009; 36(9):1377–82.
8. Leong SP, Kim J, Ross M, et al. A phase 2 study of (99m)Tc-tilmanocept in the detection of sentinel lymph nodes in melanoma and breast cancer. Annals Surgical Oncol. 2011; 18(4):961–969.
9. Wallace AM, Han LK, Povoski SP, et al. Comparative evaluation of [(99m)tc]tilmanocept for sentinel lymph node mapping in breast cancer patients: results of two phase 3 trials. Annals Surgical Oncol. 2013; 20(8):2590–2599.
10. Marcinow AM, Hall N, Byrum E, et al. Use of a novel receptor-targeted (cd206) radiotracer, 99mtc-tilmanocept, and spect/ct for sentinel lymph node detection in oral cavity squamous cell carcinoma: initial institutional report in an ongoing phase 3 study. JAMA Otolaryngology-Head & Neck Surgery. 2013; 139(9):895–902. [PubMed: 24051744]
11. Vera DR, Wallace AM, Hoh CK, et al. A synthetic macromolecule for sentinel node detection: [^{99m}Tc]DTPA-mannosyl-dextran. J Nuclear Med. 2001; 42(6):951–959.
12. Stroup SP, Kane CJ, Farchshchi-Heydari S, et al. Preoperative sentinel lymph node mapping of the prostate using PET/CT fusion imaging and Ga-68-labeled tilmanocept in a dog model. Clin Exp Metastasis. 2012; 29(7):673–680. [PubMed: 22714690]
13. Qin Z, Hall DJ, Liss MA, et al. Optimization via specific fluorescence brightness of a receptor-targeted probe for optical imaging and positron emission tomography of sentinel lymph nodes. J Biomed Optics. 2013; 18(10):101315.1–101315.12.
14. Emerson DA, Limmer KK, Hall DJ, et al. A receptor-targeted fluorescent radiopharmaceutical for multi-reporter sentinel lymph node imaging. Radiology. 2012; 265:186–193. [PubMed: 22753678]
15. Dutta R, Kluftinger A, MacLeod M, et al. Revisiting the “10% rule” in breast cancer sentinel lymph node biopsy: an approach to minimize the number of sentinel lymph nodes removed. Am J Surgery. 2012; 203(5):623–627.
16. Warncke SH, Mattei A, Fuechsel FG, et al. Detection rate and operating time required for gamma probe-guided sentinel lymph node resection after injection of technetium-99m nanocolloid into the prostate with and without preoperative imaging. Euro Urol. 2007; 52(1):126–132.
17. van der Poel HG, Buckle T, Brouwer OR, et al. Intraoperative laparoscopic fluorescence guidance to the sentinel lymph node in prostate cancer patients: clinical proof of concept of an integrated functional imaging approach using a multimodal tracer. Euro Urol. 2011; 60(4):826–833.
18. Weckermann D, Dorn R, Trefz M, et al. Sentinel lymph node dissection for prostate cancer: experience with more than 1,000 patients. J Urol. 2007; 177:916–20. [PubMed: 17296375]
19. Cheng L, Zincke H, Blute ML, et al. Risk of prostate carcinoma death in patients with lymph node metastasis. Cancer. 2001; 91(1):66–73. [PubMed: 11148561]
20. Joslyn SA, Konety BR. Impact of extent of lymphadenectomy on survival after radical prostatectomy for prostate cancer. Urology. 2006; 68(1):121–125. [PubMed: 16806432]
21. Briganti A, Karnes JR, Da Pozzo LF, et al. Two positive nodes represent a significant cut-off value for cancer specific survival in patients with node positive prostate cancer. A new proposal based on a two-institution experience on 703 consecutive N+ patients treated with radical prostatectomy, extended pelvic lymph node dissection and adjuvant therapy. Euro Urol. 2009; 55(2):261–270.
22. Ploussard G, Briganti A, de la Taille A, et al. Pelvic lymph node dissection during robot-assisted radical prostatectomy: efficacy, limitations, and complications-a systematic review of the literature. Euro Urol. 2014; 65(1):7–16.

23. Passoni NM, Abdollah F, Suardi N, et al. Head-to-head comparison of lymph node density and number of positive lymph nodes in stratifying the outcome of patients with lymph node-positive prostate cancer submitted to radical prostatectomy and extended lymph node dissection. Urologic Oncol. 2014; 32(1):29, e1–e8.

24. Abdollah F, Suardi N, Cozzarini C, et al. Selecting the optimal candidate for adjuvant radiotherapy after radical prostatectomy for prostate cancer: a long-term survival analysis. Euro Urol. 2013; 63(6):998–1008.

25. Gandaglia G, Trinh QD, Hu JC, et al. The impact of robot-assisted radical prostatectomy on the use and extent of pelvic lymph node dissection in the “post-dissemination” period. Euro J Surgical Oncology. 2014 Jan 02. EPub ahead of print.

26. Abdollah F, Abdo A, Sun M, et al. Pelvic lymph node dissection for prostate cancer: adherence and accuracy of the recent guidelines. Intl J Urol. 2013; 20(4):405–410.

27. Lyman GH, Giuliano AE, Somerfield MR, et al. American Society of Clinical Oncology guideline recommendations for sentinel lymph node biopsy in early-stage breast cancer. J Clinical Oncol. 2005; 23(30):7703–7720. [PubMed: 16157938]

28. Mattei A, Fuechsel FG, Bhatta Dhar N, et al. The template of the primary lymphatic landing sites of the prostate should be revisited: results of a multimodality mapping study. Euro Urol. 2008; 53(1):118–125.

29. Godoy G, Chong KT, Cronin A, et al. Extent of pelvic lymph node dissection and the impact of standard template dissection on nomogram prediction of lymph node involvement. Euro Urol. 2011; 60(2):195–201.

30. Briganti A, Chun FK, Salonia A, et al. Complications and other surgical outcomes associated with extended pelvic lymphadenectomy in men with localized prostate cancer. Euro Urol. 2006; 50(5): 1006–1013.

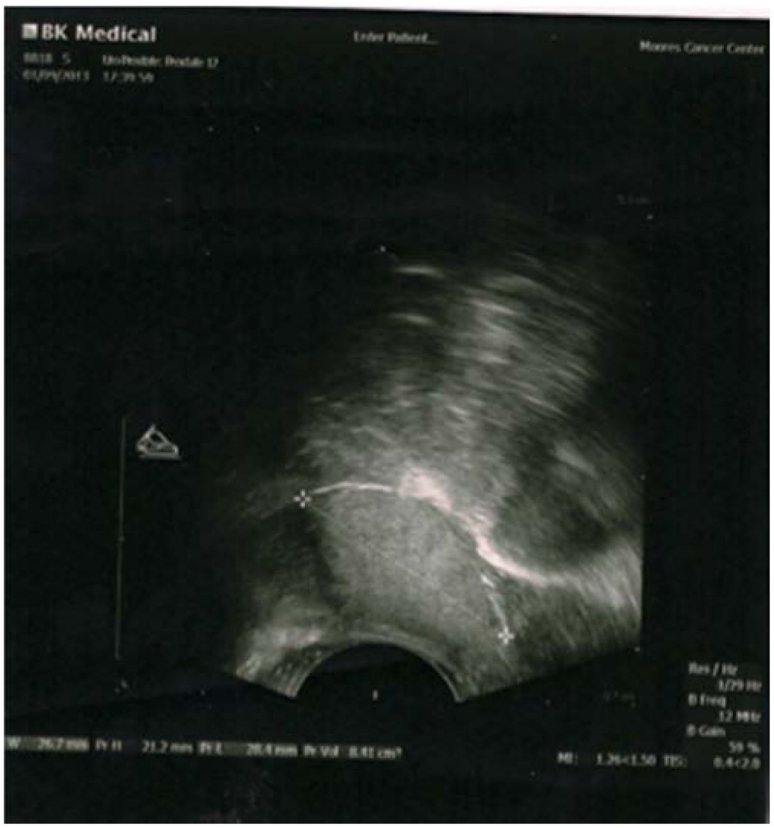

Figure 1.
Prostate Ultrasound demonstrating (**A**) an 8cc gland and a (**B**) guided needle injection (yellow arrow).

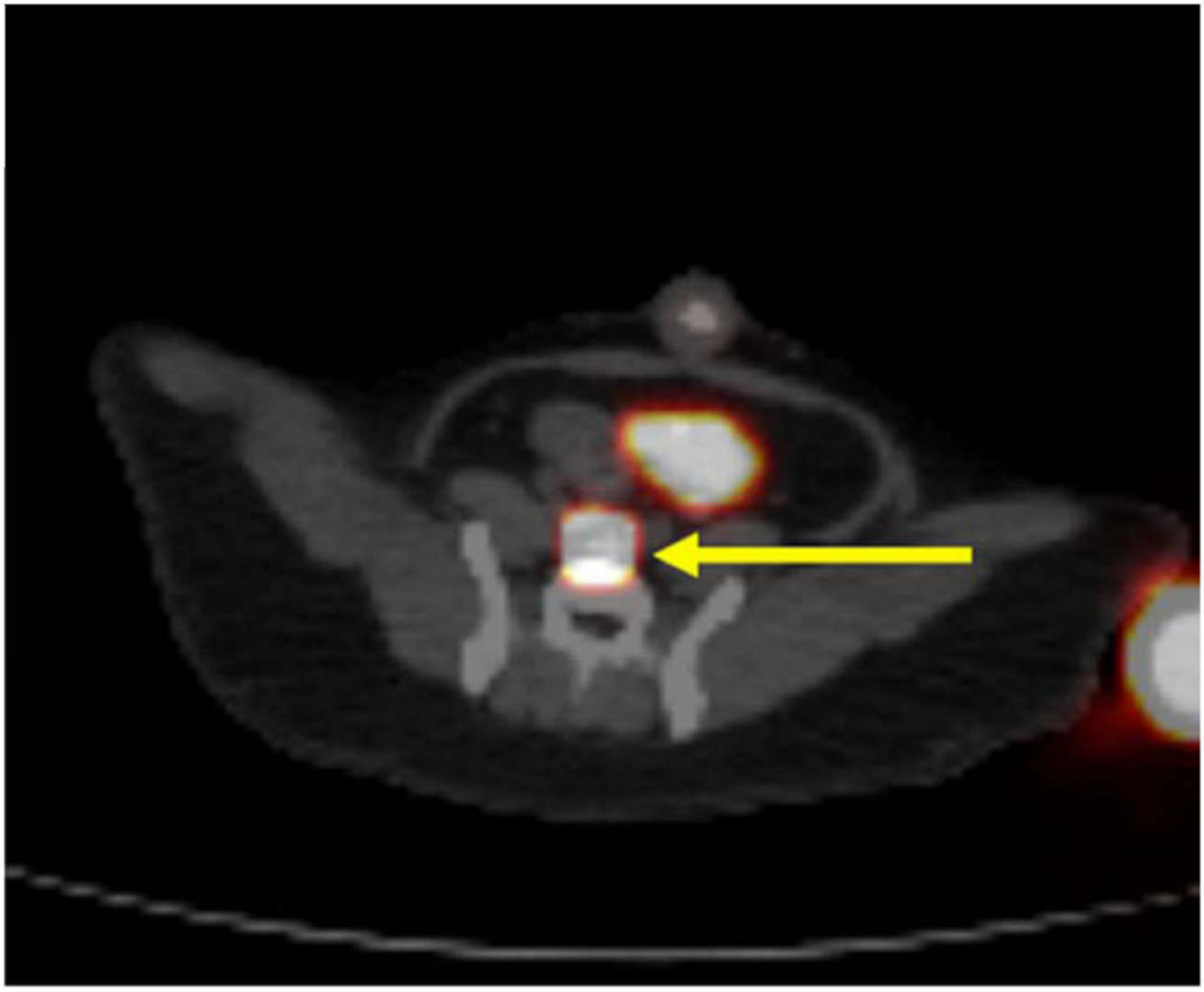

Figure 2.
Coronal view of PET/CT scan noting a coronal cross-section (**A**) of presacral sentinel lymph node (yellow arrow), (**B**) the axial and (**C**) sagittal cross-sections of the same sentinel lymph node.

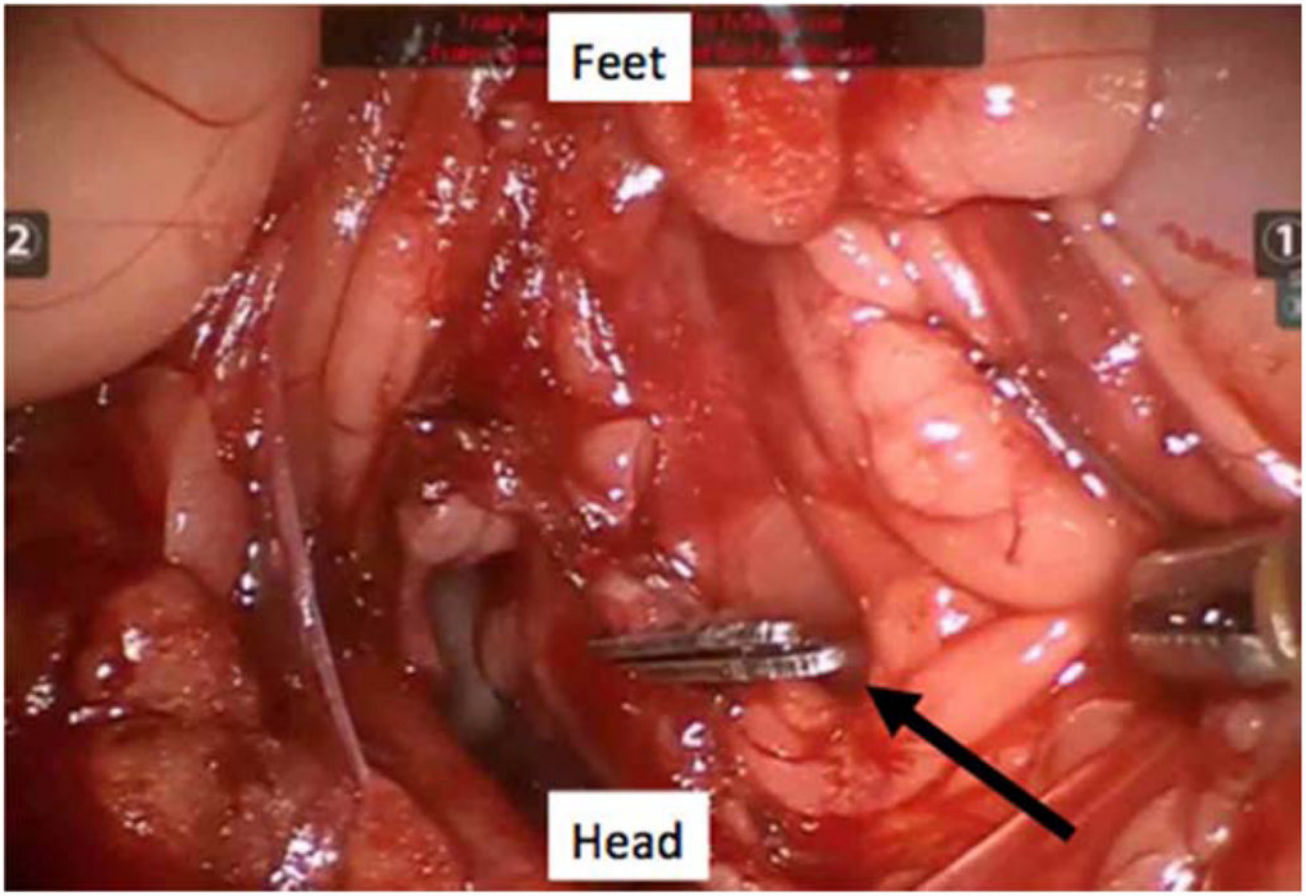

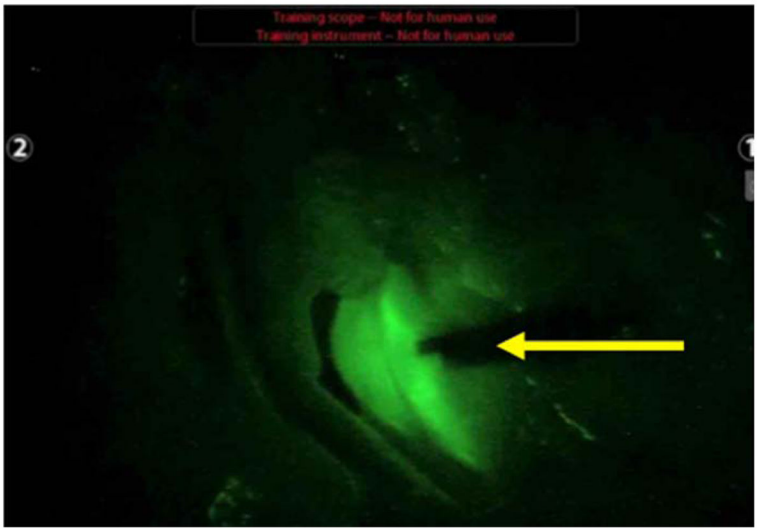

Figure 3.

Intraoperative FireFly™ Robotic Surgical camera view looking into the pelvis as a normal robotic prostatectomy view noting a presacral sentinel lymph node (clip designated with

black arrow) with (**A**) the fluorescence mode off and (**B**) with the fluorescence mode on (clip designated with yellow arrow).

Table 1

Sentinel lymph node accumulation during PET/CT and visualization during robotic surgery

	Experiment								
	One			Two			Three		
Nodes/Tissues	**SUV**	**Satisfy 5% rule (Yes/No)**	**in vivo fluorescence (Yes/No)**	**SUV**	**Satisfy 5% rule (Yes/No)**	**in vivo fluorescence (Yes/No)**	**SUV**	**Satisfy 5% rule (Yes/No)**	**in vivo fluorescence (Yes/No)**
L. External iliac		No	No		No	No		No	No
L. common Iliac	1	Yes	Yes	14.1	Yes	Yes	4.1	Yes	Yes
Presacral	12.9	Yes	Yes	66.3	Yes	Yes	20.5	Yes	Yes
Pariaortic	2	Yes	Yes	9.0	Yes	Yes		Yes	Yes
R external iliac		No	No		No	No		No	No
R. common iliac	85	Yes	Yes	4.4	Yes	Yes	5.4	Yes	Yes

SUV = Standardized Uptake Values obtained from PET/CT imaging

Urology. Author manuscript; available in PMC 2015 October 01.